



City Research Online

## City, University of London Institutional Repository

---

**Citation:** Abdelmalik, A. A., Fothergill, J. & Dodd, S. J. (2012). Electrical Conduction and Dielectric Breakdown Characteristics of Alkyl Ester Dielectric Fluids obtained from Palm Kernel Oil. *IEEE Transactions on Dielectrics and Electrical Insulation*, 19(5), pp. 1623-1632. doi: 10.1109/tdei.2012.6311509

This is the accepted version of the paper.

This version of the publication may differ from the final published version.

---

**Permanent repository link:** <https://openaccess.city.ac.uk/id/eprint/13248/>

**Link to published version:** <https://doi.org/10.1109/tdei.2012.6311509>

**Copyright:** City Research Online aims to make research outputs of City, University of London available to a wider audience. Copyright and Moral Rights remain with the author(s) and/or copyright holders. URLs from City Research Online may be freely distributed and linked to.

**Reuse:** Copies of full items can be used for personal research or study, educational, or not-for-profit purposes without prior permission or charge. Provided that the authors, title and full bibliographic details are credited, a hyperlink and/or URL is given for the original metadata page and the content is not changed in any way.

---

City Research Online:

<http://openaccess.city.ac.uk/>

[publications@city.ac.uk](mailto:publications@city.ac.uk)

---

# Electrical Conduction and Dielectric Breakdown Characteristics of Alkyl Ester Dielectric Fluids obtained from Palm Kernel Oil

A.A. Abdelmalik, J.C. Fothergill, and S.J. Dodd

Department of Engineering  
University of Leicester  
Leicester, U.K.

## ABSTRACT

Naturally-occurring palm kernel oil (PKO) and its ester derivatives are being considered as sustainable alternatives to synthetic oils for use as dielectric fluids. This paper reports on their dielectric properties, which have been studied and compared to BS148 mineral oil. The low frequency complex dielectric response of the PKO and its derivatives are related to ionic conduction and electrode polarization phenomena. The purified PKO has an electrical conductivity of  $3.04 \times 10^{-12}$  at 30°C; this is 10 times lower than crude PKO but about 10 times greater than the BS148 oil. The bulk conductivity is thermally activated, activation energy = 0.47 eV, and influenced by viscosity. The ester derivatives had a higher conductivity than the PKO, which was related to ionic impurities introduced during processing. The breakdown field was measured in a bespoke cell enabling smaller volumes of oil (15 ml) than that used in ASTM D1816. The characteristic AC breakdown strength of purified PKO and its alkyl esters were found to be in the range, 41 to 43 kV/mm, which is significantly higher than the mineral oil (27 kV/mm). The results support the proposition that a dielectric fluid derived from palm kernel oil, once re-purified, may be a suitable replacement for mineral oil based fluids in HV electrical equipment.

Index Terms — palm kernel oil, ester derivatives, dielectric loss, viscosity, AC characteristic breakdown field, Weibull distribution.

## 1 INTRODUCTION

Environmental sustainability provides an impetus to search for alternative high performance insulation fluids for use in electrical equipment<sup>1</sup>. Such alternatives include processed ester derivatives of crude palm kernel oil<sup>2</sup>. The challenge here is to produce an insulating oil that can be used over a wide range of temperatures. In the case of crude palm kernel oil, with about 83% saturated fatty acids and 17% unsaturated fatty acids, significant chemical processing such as purification and transesterification is necessary to reduce the pour point temperature. In transformers, such fluids are intended to improve the dielectric strength of the insulation papers and must provide insulation between the live and grounded parts. They must also enable efficient heat transfer and dissipation through conduction and convection. It is therefore necessary for an alternative oil to have as good a performance as existing mineral oil in terms of its electrical and flow properties. Of particular concern are the electrical conductivity, the dielectric breakdown strength, and the dynamic viscosity of the dielectric liquids.

In this paper, measurements of the dielectric permittivity,

electrical conductivity, breakdown strength and dynamic viscosity of raw and purified vegetable oils, and their ester derivatives are reported and compared with mineral oil (BS148). As breakdown strength measurements depend strongly on the electrode arrangement and the apparatus used<sup>3</sup>, and because only small volumes of the processed derivatives could be easily synthesized using the current laboratory based apparatus, it was necessary to design a new bespoke breakdown test cell that was had a lower sample volume than the standard breakdown test cell<sup>4</sup>. In order to validate the new test cell in terms of obtaining breakdown results that are comparable with the standard technique and to establish reliability of the measurement, the breakdown strength of mineral oil, measured using the new bespoke cell, was compared to literature values measured using the ASTM D1816 standard. The breakdown strength distributions of the ester derivatives were then measured using the bespoke cell and compared using Normal and Weibull statistics.

### 1.1 DIELECTRIC PROPERTIES

Dielectric fluids used as electrical insulators in power equipment are mainly non-polar, although the application of an electric field may result in the formation of induced dipoles.

The applied electric field may also lead to the dissociation of impurities and the consequent formation of mobile ions. At low frequencies, the dielectric loss is dominated by conduction due to the drift of such charged particles. Mobile charge carriers may accumulate at the liquid-electrode interface under an applied electric field to form an electrical double layer, which can be described by the Gouy-Chapman model<sup>5</sup>, since the dissociable impurity in the liquid behaves as a weak electrolyte<sup>6</sup>. The thickness of the layer depends on the applied electric field, the temperature of the liquid, and the concentration of the mobile charge carriers in the liquid<sup>5</sup>. There exists an interplay between (i) the electrostatic forces between mobile charges and those on the electrode surface, and (ii) the thermal agitation of the molecules randomizing the position of the mobile charges. The electrostatic forces tend to overcome the thermal processes at the interface leading to a diffuse layer of charge of finite thickness. With increasing concentrations of mobile charges, this diffuse electrical double layer becomes thinner and will lead to an increase in the real part of the measured relative permittivity of the sample at low frequency. The double layer created by the accumulated charges under an alternating electric field leads to interfacial relaxation (Maxwell-Wagner) dielectric behavior at low frequencies<sup>6</sup>. The characteristic thickness of the region where the charges are distributed is dependent on the temperature of the liquid and the concentration of the charge carriers. These parameters are related with the expression<sup>5</sup>,

$$t_{DL}^2 = \frac{\epsilon kT}{2nz^2e^2} \quad 1$$

where  $t_{DL}$  is the characteristic thickness of the diffuse layer,  $n$  is the number density of mobile charge carriers,  $z$  is the charge valence,  $e$  is the elementary charge,  $\epsilon$  is the permittivity of the liquid,  $k$  is the Boltzmann constant and  $T$  is absolute temperature. The dielectric loss resulting from the polarization mechanisms and the bulk conductivity of the liquid is expressed as<sup>7</sup>:

$$\tan \delta(\omega) = \frac{\epsilon''(\omega) + \sigma_o / \epsilon_o \omega}{\epsilon_r'(\omega)} \quad 2$$

where  $\epsilon_r'(\omega)$  and  $\epsilon''(\omega)$  are the real and imaginary components of the relative permittivity of the liquid as a function of angular frequency and  $\sigma_o$  is the DC conductivity. An effective AC conductivity may be defined as the ratio of the dissipated power to the square of the magnitude of the field at a given frequency arising from conduction and dipole orientation losses; this may be expressed as<sup>8</sup>:

$$\sigma_{ac}(\omega) = \omega \epsilon_o \epsilon''(\omega) + \sigma_o \quad 3$$

Since the dielectric fluids in question are mainly non-polar, the AC conductivity is dominated by the DC conductivity rather than the dielectric polarization loss. The DC conductivity of the liquid is given by

$$\sigma_o = \sum_i n_i \mu_i \quad 4$$

where  $\mu_i$  is the mobility for charge carrier of type  $i$ ,  $n_i$  is the concentration for the charge carrier of type  $i$ , and the summation is over all mobile charge carrier types. The capacitance of the electric double layer can be determined if the layer is modeled to be a capacitor (representing the double layer) in series with a parallel RC network (representing the polarization and bulk dc conductivity of the oil

Due to the small thickness of the double layer, a high electric field will exist within the double layers at the electrodes. This will lead to electron injection from the cathode and the field-aided dissociation of liquid molecules and impurities, resulting in the production of additional free ionic charge carriers that are required for maintaining the DC conduction through the bulk of the liquid.

## 1.2 DYNAMIC VISCOSITY

Fluids resist the relative motion of objects immersed in them. Movement of ions, as well as the motion of layers of the liquid having different velocities within them depends on the dynamic viscosity of the liquid. Most dielectric liquids hinder ionic movements due to their large molecular size composition<sup>9</sup>. Increase in temperature most often results in decrease in the viscosity of liquid, thereby reducing the resistance of the charge carriers to move. This can lead to an increase in the concentration and mobility of mobile charge carriers, and in turn, an increase in the electrical conductivity and dielectric loss of the liquid. The electrical conductivity of a dielectric liquid is therefore dependent on the concentration of mobile charge carriers and the viscosity.

## 1.3 DIELECTRIC BREAKDOWN

Under sufficiently high applied electric fields, the dielectric liquid will breakdown. The processes of electrical breakdown in dielectric liquids are not fully understood. However a number of processes have been identified which may contribute to breakdown. The types of breakdown process depend on the existence or otherwise of regions of field non-uniformity due to material interfaces having complex geometry. In addition, dielectrophoresis may cause uncharged particles to move to regions of high electric field further increasing the inhomogeneity and the additional electric field enhancement. If the particles have a higher  $\epsilon_r'$  than the oil at the power frequency then the particles will move towards the higher field region, otherwise they will move away<sup>10</sup>. As ionic charge carriers, responsible for the dc electrical conductivity, drift and collide with liquid molecules, momentum is lost and energy is transferred to the fluid leading to electrohydrodynamic (EHD) motion of the liquid near breakdown<sup>11</sup>. This turbulent motion in oil between the electrodes causes the temperature of the liquid to rise locally. It also significantly affects the local pressure<sup>12</sup>. The injected energy could also result in a phase change in the oil or liberation of simpler molecules from the dissociation of part of the oil molecule. The liberated vapor influences the formation of bubbles<sup>13</sup>. Discharges may take place when the electric field in a spherical gas bubble becomes equal to the gaseous ionization field, which will lead to decomposition of the liquid and breakdown may follow<sup>14</sup>. Intrinsic breakdown

may occur if the conduction ions gain energy from the field as they drift through the liquid; some of this kinetic energy is lost as a result of collisions with the liquid molecules. The energy gained by the liquid molecules may lead to excitation of C–H and C–C bonds and may result in some of the bonds being broken thereby producing extra ions<sup>13</sup>.

Breakdown measurements of liquids and solids result in a distribution of values due to the stochastic nature of the breakdown mechanism. There may also be variations due to the measurement technique and variations in impurity concentrations, etc. In ASTM1816, the withstand voltage is usually expressed as the mean value of breakdown voltage of a number of breakdown measurements of the material. The standard deviation of the data is used to evaluate the spread of the data values around the mean value. As suggested in IEEE 930-2004, the Normal distribution is not usually appropriate for the analysis of electrical breakdown data, Weibull statistics are more commonly used. Weibull statistics are reported to have wide applicability for breakdown measurements of liquids and solids and are based on an extreme value distribution in which the system fails when the weakest link fails<sup>15</sup>. Martin et al evaluates the effectiveness of esters as dielectrics using statistical analysis of the withstand voltages of ester based transformer fluids in comparison with mineral oil. They reported that the Weibull distribution is appropriate for the evaluation of withstand voltage of transformer oils<sup>16</sup>. The measurement of electrical breakdown strength of an electrical insulating liquid is usually carried out under progressive stress regime where the applied voltage is increased with time either under a stepped increase or a continuous increase (ramp) until breakdown of the sample occurs. This is measured for a number of breakdowns and the characteristic breakdown field of the insulating liquid can be estimated from the dispersion of the breakdown field data<sup>17</sup>. The cumulative probability of failure for the two-parameter Weibull distribution is given by equation 5.

$$F(v) = 1 - \exp\left\{-\left(\frac{v}{\alpha}\right)^\beta\right\} \quad 5$$

where  $F(v)$  is the cumulative probability of breakdown at voltage,  $v$ ,  $\alpha$ , the characteristic breakdown voltage is the value of  $v$ , at which the cumulative probability of failure is  $(1 - \exp\{-1\}) = 0.632$ , and  $\beta$ , is the shape parameter, which is a measure of the range of failure voltages within the distribution<sup>15</sup>. The estimation of the characteristic breakdown strength, the shape parameters, and the confidence bounds of the distribution describing an insulating fluid can be used to evaluate the characteristics of the fluid following synthesis and can also be used for quality control.

## 2 EXPERIMENTAL

### 2.1 MATERIALS

Specimens of BS148 mineral insulating oil were prepared

and dried by degassing in a vacuum oven at a temperature of 85°C for 2 hours. Crude palm kernel oil (CPKO) was purchased from Jarmac Ltd and was purified using the W. R. Grace<sup>18</sup> Modified Physical Refining Process (MPR) for treating glyceride oils. The purified oil samples (PPKO) were then degummed, neutralized and treated with 1% Silica gel (Grace Davison Trysil 300) and 10% tonsil Acidified clay. Alkyl ester of palm kernel oil (PKOAE) was synthesized from the purified oil by transesterification. Epoxy alkyl ester (PKOEAE) was then synthesized by epoxidation of the palm kernel oil alkyl ester<sup>2</sup>. All ester derivatives were dried using the same method as employed for mineral oil.

### 2.2 DIELECTRIC RESPONSE AND DC CONDUCTIVITY

The dielectric properties of the liquid samples were tested in a specially designed test cell. The voltage electrodes consist of two steel disks on either side of the measurement electrode. The measurement electrode consists of a steel disc surrounded by a guard electrode. Glass beads were used as spacers to maintain an electrode gap of 1mm between the two voltage electrodes and measurement electrode. The two voltage electrodes are connected electrically via a clamping screw. Using this

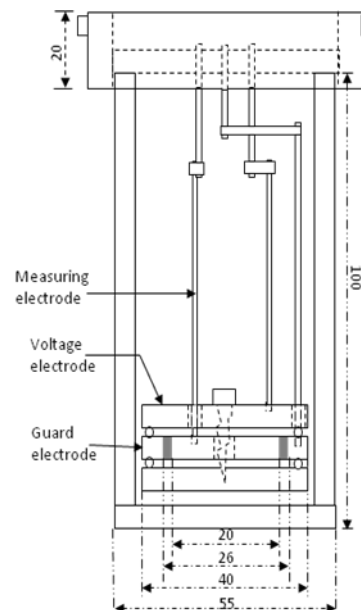


**Figure 1: Bespoke three electrode test cell for dielectric measurements (The dimensions are in mm)**

arrangement doubles the effective area of the electrode system, shown in figure 1. The capacitance of the cell in free space was 8.04 pF. The cell was placed in a heated water bath equipped with a temperature controller to control the temperature of the sample. Brass rods were used to form the electrical connections to the guard, measurement and voltage electrodes. The cell electrodes were connected to a Solartron 1255 Frequency Response Analyzer and 1296 Dielectric Interface and controlled by a desktop computer in order to measure the dielectric response of the sample. Dielectric measurements

were taken over the frequency range  $10^{-3}$  Hz to 100 Hz and at a number of fixed temperatures within the range 20°C to 90°C. For DC conductivity measurements, the current flowing through the samples was determined using Kiethley 6430 picoammeter. The current was reasonably stable after 1 minute and final measurements were made after 15 minutes.

## 2.3 VISCOSITY/DENSITY MEASUREMENT

The dynamic viscosity is defined as the ratio of the applied shearing stress to the rate of shear of a fluid and is measured in Pa.s. The kinematic viscosity of the fluids was determined using a suspended-level capillary viscometer of calibration constant  $2.518 \times 10^{-2}$  cSt/sec. The viscometer was placed in a temperature controlled water bath allowing measurements to be obtained at different temperatures between 20°C and 60°C. The measurement of viscosity involves measurement of the time taken for a fixed volume of the liquid to flow through a narrow capillary and a multiplication by the calibration constant. Samples were introduced into the reservoir carefully to avoid gas bubbles. The dynamic viscosity in cP was calculated from the kinematic viscosity by dividing by the density of the oil sample and in SI units of Pa.s by multiplying by a conversion factor of 1000.

The density of the samples was determined using a Paar DMA 40 digital density meter. This consists of a U-tube glass capillary having a natural mechanical resonant frequency. When a sample of liquid is drawn into the capillary, the resonant frequency changes by an amount dependent on the density of the liquid. To control the temperature the capillary is mounted in the centre of a double walled glass cylinder, with the inner cavity filled with a gas of high thermal conductivity and the outer cavity having water supplied from a thermostatically controlled water bath. For each measurement, the U-tube was completely filled with the sample taking care not to introduce any bubbles. The relative density of the sample was evaluated from the measured oscillation period of the capillary first containing air and then the dielectric fluid.

## 2.4 BREAKDOWN APPARATUS

The breakdown test setup, as shown in figure 2, consists of a transformer control unit (TCU), a variable transformer (variac), and a 240 V/50 kV step-up transformer with a low voltage secondary tap to monitor the applied voltage using a multimeter, V. A current limit resistor, R, was also connected in series with the sample cell. The TCU monitors the cell current and interrupts the supply voltage to the step-up transformer when breakdown occurs in the sample cell. During each experiment the applied voltage was increased from zero at a rate of approximately 0.4 kV/s until breakdown occurred. The test cell was designed to take small sample volumes ( $\approx 5$ ml) compared to the volume required using the IEC 156:1995 standard designed cell (350 ml to 600 ml). The cylindrical test cell, shown in figure 2, was made from a Perspex (Poly(methyl methacrylate)) tube to host the oil sample and the electrodes. The electrodes consist of two stainless steel spheres of radius 12.5 mm each in contact with a brass rod to provide an electrical connection. An internal Perspex tube was used

between the sphere electrodes to give a minimum electrode gap of 1 mm along the centre axis of the cell. The maximum electric field strength between the spherical electrodes was evaluated using Cloete and van der Merwe's method<sup>9</sup> for two conducting spheres using the method of images. The electric field enhancement over a plane-plane electrode system was calculated to be 2.68%. This small field enhancement was due to the radius of the electrodes being much greater than the inter-electrode gap<sup>19</sup>. For each oil sample of CPKO and PPKO, five breakdown measurements were carried out at 30°C, i.e. at a temperature greater than the pour point temperature. In each case of the processed oils (PKOAE and PKOEAE), and for mineral oil, all having significantly lower pour-point temperatures, breakdown measurements were carried out at 20°C.

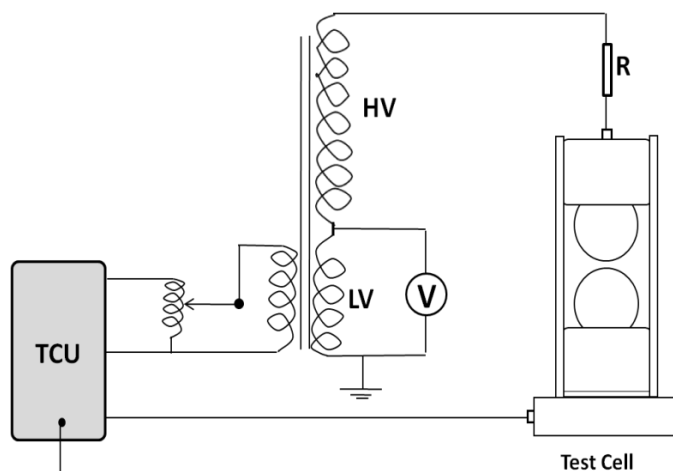


Figure 2: Schematic of electric breakdown test setup and bespoke breakdown test cell.

## 3: RESULTS AND DISCUSSION

### 3.1 DIELECTRIC RESPONSE

The dc electrical conductivity of the CPKO and PPKO samples obtained at 30°C, and the other samples PKOAE, PKOEAE and BS148 at 20°C, are shown in Table 1. The dc conductivity of the crude palm kernel oil was found to decrease by a factor of approximately 10 after purification. The purified oil, PPKO, was found to have a conductivity of approximately 10 times that of BS148 mineral oil. However, the alkyl esters were found have an increased conductivity compared with PPKO, this may be related to high mobility of the charged particles due to low viscosity of the esters or due to increased ionic impurities introduced during processing. The dielectric properties of the crude and processed oils are shown in figures 4, 5 and 6. Figures 3 and 4 show the real and imaginary components of permittivity as a function of frequency (i.e. a Bode plot) for CPKO, PPKO, PKOAE, and PKOEAE measured at the highest temperature of 80°C. Above the frequency of approximately  $10^{-2}$  Hz in the case of CPKO and PPKO and above the frequency of  $10^{-1}$  Hz in the case of the processed oils (PKOAE and PKOEAE), the real part is constant (i.e. independent of frequency) and the imaginary part is inversely proportional to frequency. This is

symptomatic of a constant capacitance in parallel with a dc conductance – i.e. a dc electrical conduction mechanism dominates in this frequency range. At lower frequencies, the real part acquires a negative slope of greater than -1, whilst the imaginary part maintains a slope of -1. This is indicative of Maxwell-Wagner interfacial polarization<sup>20</sup>. In order to

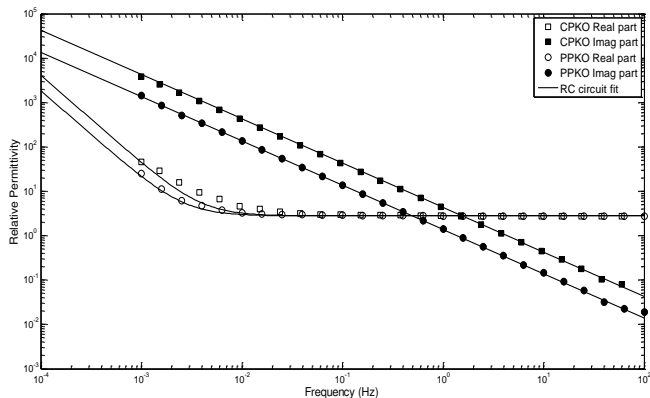


**Figure 3: Real and imaginary parts of the dielectric permittivity and fitted equivalent circuit model for the dielectric fluids CPKO and PPKO measured at 80 °C**

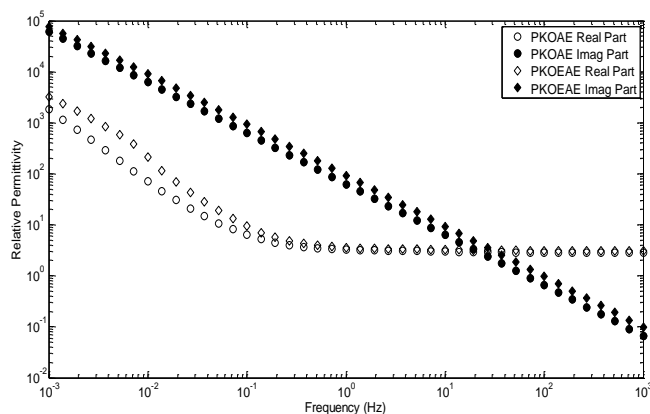


**Figure 4: Real and imaginary parts of the dielectric permittivity for the dielectric fluids PKOAE and PKOEA measured at 80 °C**

represent this data, the equivalent circuit of the form shown in figure 5 is proposed for the dielectric response of purified palm kernel oil. The equivalent circuit consists of two series capacitors,  $C_{DL}$ , representing non-conducting electric double layers at the electrode connected in series with a parallel combination of  $C_L$  and  $R$  representing polarization and bulk

conduction of the liquid.

The equivalent circuit parameters were estimated to give a best fit to the data of figure 3. The fitted response is shown as the solid lines in figure 3. The corresponding  $\tan\delta$  curve is shown in figure 6 and enables the relaxation frequency of the Maxwell-Wagner response to be determined.

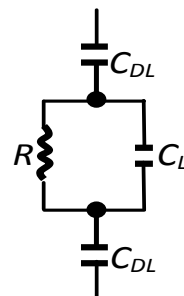


**Figure 5: Equivalent circuit used to represent the experimental data shown in figure 3.**

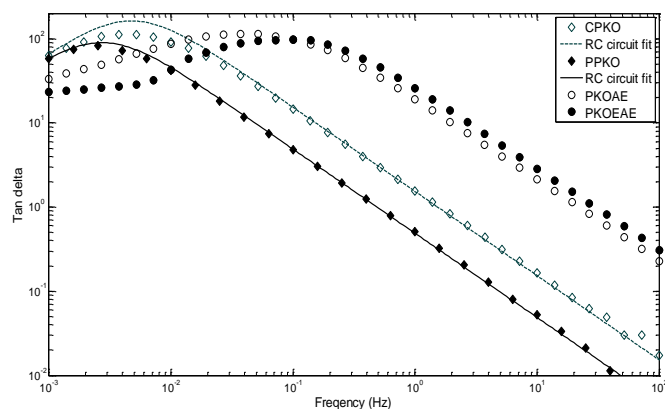


**Figure 6:  $\tan\delta$  curve of PKO-based dielectric fluids and fitted equivalent circuit model for the CPKO and PPKO at 80 °C**

Close inspection of the experimental and the model data from the crude and purified oil and the fitted model data in figure 6 reveals a better fit for the PPKO liquid than the CPKO experimental data, especially for the data points close to the relaxation peak. The equivalent circuit model has a simple Debye type relaxation. Hence the data suggests that the response from PPKO better conforms to a Debye type relaxation while the response for CPKO differs significantly from a simple Debye process. The broader peak in the behavior of CPKO may be related to a distribution of relaxation times arising from the transport of different types of impurity charge

**Table 1 : Conductivity and Viscosity Characteristics**

Samples	$\sigma_{DC}$	$\sigma_{AC}$	Activation Energy for $\sigma_{AC}$ (eV)	Viscosity (cSt)	Activation Energy for Viscosity (eV)
BS148	$2.60 \times 10^{-13}$	$4.6 \times 10^{-13}$	0.45	21	0.32
CPKO	$5.51 \times 10^{-11}$	$3.01 \times 10^{-11}$	0.33	44	0.28
PPKO	$3.40 \times 10^{-12}$	$4.35 \times 10^{-12}$	0.47	44	0.28
PKOAE	$1.18 \times 10^{-10}$	$3.96 \times 10^{-10}$	0.27	3.2	0.17
PKOEA	$1.06 \times 10^{-9}$	$1.68 \times 10^{-9}$	0.18	4.8	0.19

Note: Values for CPKO and PPKO are at 30 °C, while the values for BS148, PKOAE and PKOEA are at 20 °C

carriers. Frequency response measurement represents a spatial average measurement over the volume of the sample. This leads to a spread in relaxation times with a distribution centered on the most probable value<sup>21</sup>. This is an indication that CPKO contains a greater variety of impurities leading to greater overall conductivity and a greater distribution of relaxation times. Hence, processing of the crude oil to form PPKO has reduced the number and variety of impurities in the oil. The greater bulk conductivity of CPKO also leads to a peak in  $\tan\delta$  at a higher frequency compared with PPKO. The  $\tan\delta$  peaks of PKOAE and PKOEAE shift towards a higher frequency consistent with their greater bulk dc conductivity. The equivalent circuit did not fit the ester derivatives of palm kernel oil, suggesting that more complex charge transport processes may be involved at the electric double layer.

The ac electrical conductivities determined from the slope of the imaginary part of the frequency response data,  $\sigma_{AC}$ , for CPKO, PPKO, PKOAE and PKOEAE within the temperature range of 20 to 90°C are plotted on Arrhenius axes in Figure 7. The straight lines obtained indicate thermally activated transport mechanisms. The activation energies of CPKO, PPKO, PKOAE and PKOEAE derived are shown in Table 1. Over the temperature range 20 to 90°C, the electrical conductivity of the palm kernel oil was found to decrease by a factor of approximately 10 after purification but significantly increase on further processing of the oil reflecting the same behavior seen in the dc conductivity results. The electrical conductivity is therefore a thermally activated process with higher activation energy found in the samples with lower concentration of mobile impurities.

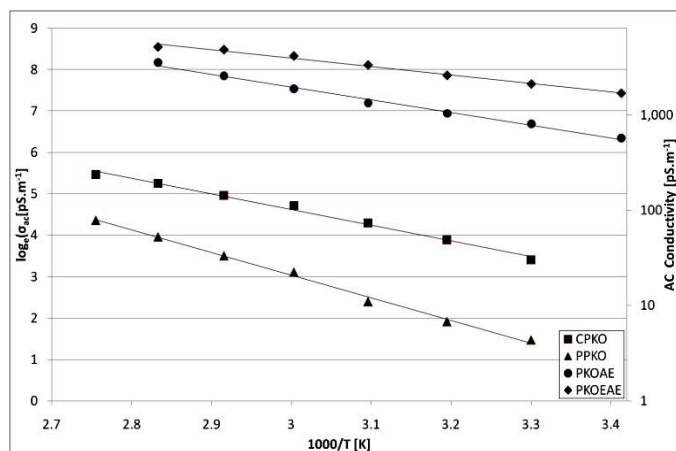


Figure 7: Arrhenius Plot for Electrical Conductivity of Oil samples

### 3.2 VISCOSITY MEASUREMENTS

The conductivity of a liquid is known to be dependent on the concentration and mobility of ions within the liquid. The transport of ions and hence their mobility will be influenced by the dynamic viscosity of the liquid<sup>21</sup>. Figure 8 shows the dynamic viscosity of the purified palm kernel oil, PPKO, and the ester derivatives, PKOAE and PKOEAE on Arrhenius axes. The straight lines show that viscosity follows an activated

behavior and the derived activation energies are given in Table 1. The splitting of the oil to its respective fatty acids has significantly reduced the fluid's resistance to flow as evident from the viscosity shown in Table 1. Epoxidation of the ester derivative causes a slight increase in viscosity. There is also a significant reduction in the activation energy following transesterification indicating that the intramolecular interaction between the oil molecules is very different.

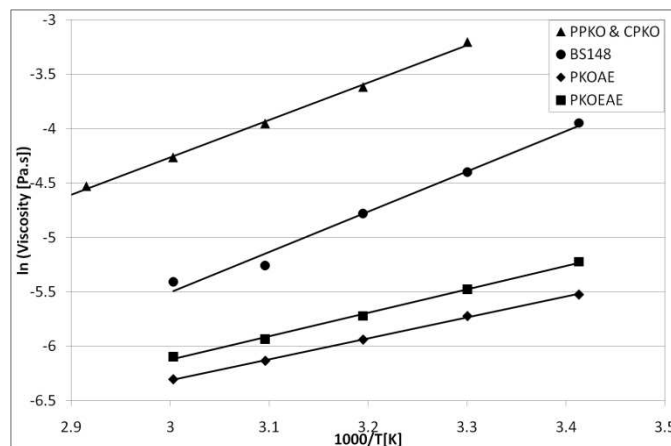


Figure 8: Arrhenius Plot for Viscosity of the Oil Samples

The relationship between the electrical conductivity and dynamic viscosity was investigated. In figures 9 and 10 the ac conductivity is plotted as a function of the inverse of dynamic viscosity of the crude and different processed oils. There is a straight line fit between the electrical conductivity of CPKO and the inverse of dynamic viscosity whilst the activation energy for conductivity and viscous flow of CPKO are 0.33 eV and 0.29 eV respectively. The inverse relationship and the close values of the activation energies suggest that electrical conductivity of CPKO is determined by its viscosity. Increase in the fluidity of the impurity rich sample leads to an increase in the mobility of the charge carriers and hence the electrical conductivity. The purified PPKO sample slightly deviates from the linear relationship indicating that conductivity is not simply controlled by oil viscosity. Comparison of the activation energies of conductivity and viscous flow indicates that conductivity of the alkyl esters is viscosity dependent.

### 3.3 DIELECTRIC BREAKDOWN

The results on the analysis of breakdown tests using Normal statistics of the CPKO, PPKO, PKOAE, PKOEAE, and BS148 samples are summarized in Table 2. The mean breakdown voltage of mineral oil, 26.4 kV, with standard deviation of 1.8 kV, obtained with the bespoke breakdown test cell, is comparable with the breakdown voltage of mineral insulating oil reported in literature using the standard ASTM test cell. Insulating oil in electric equipment with voltage rating of 345 kV and above was reported to have a breakdown voltage of 26 kV<sup>22</sup>. The standard deviation of 1.8 kV is approximately 7% of the breakdown strength value and is less than the percentage of standard deviation of breakdown strength as recommended in ASTM D1816; that it should not exceed 10%. The

breakdown results obtained using the bespoke test cell demonstrates good correspondence with the ASTM test method therefore validating the use of the bespoke cell for breakdown measurements. Also shown in Table 2, are the results obtained from the crude and processed oils. The mean breakdown voltages for crude oil, 36.7 kV, increases to 40.6 kV on purification and increase further to 42.6 kV following epoxidation. The standard deviations for the breakdown strengths are similar to that obtained from the mineral oil indicating good reproducibility in the data. In table 2, the mean breakdown strength of palm kernel oil samples were compared with the minimum mean breakdown voltage recommended in the literature for natural ester (as-received) insulation fluid measured using standard test methods ASTM D1816. A natural ester based dielectric fluid is recommended to have a minimum mean breakdown voltage of 35 kV (1 mm gap) for voltage class of 345 kV and above<sup>23</sup> However, in this study the mean breakdown voltage for the PPKO, PKOAE, and PKOAEAE all have a breakdown voltage that exceeds this limit by a significant amount.

**Table 2: Normal Distribution parameters of BDV Test**

Samples	No. of Breakdowns	Mean BDV (kV)	Standard Deviation (kV)
BS1148	5	26.44	1.83
CPKO	5	36.66	1.03
PPKO	5	40.55	1.79
PKOAE	5	42.19	1.41
PKOAEAE	5	42.58	0.98

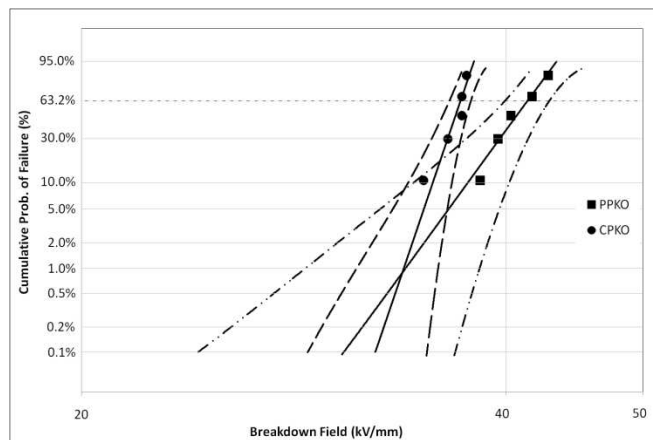


**Figure 11: Weibull plot for samples of palm kernel oil and its derivatives**

The fitted Weibull parameters of the AC breakdown field data of the oil samples, obtained using the bespoke test cell, are shown in Table 3. The characteristic breakdown strength,  $\alpha$ , and the shape parameter,  $\beta$ , are tabulated along with their respective 95% confidence bounds. The correlation coefficients of the breakdown data when fitted to the Weibull function, equation 6, are much greater than the critical correlation coefficient of  $R^2 = 0.895$  for 5 breakdowns<sup>17</sup>. As demonstrated

using Normal statistics, there is also a significant difference in the characteristic breakdown strength of CPKO when compared to the purified oil samples. This again shows that purified palm kernel oil and the alkyl ester derivatives have improved breakdown strengths. The characteristic electric field strength of the palm kernel oil ester derivatives was about 37% higher compared with BS148 mineral insulating oil.

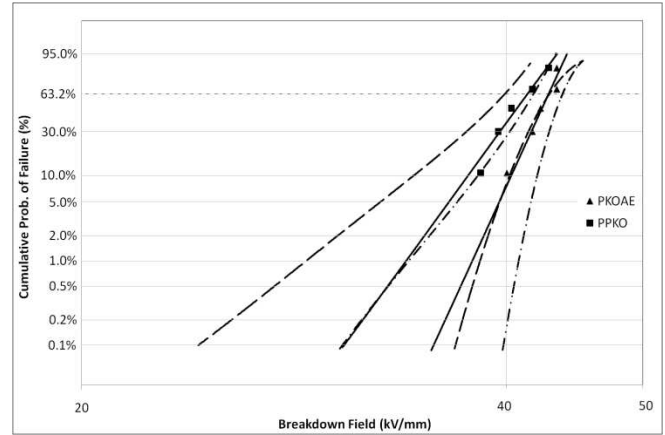


**Figure 12: Weibull plot for samples of purified palm kernel oil and its alkyl ester**

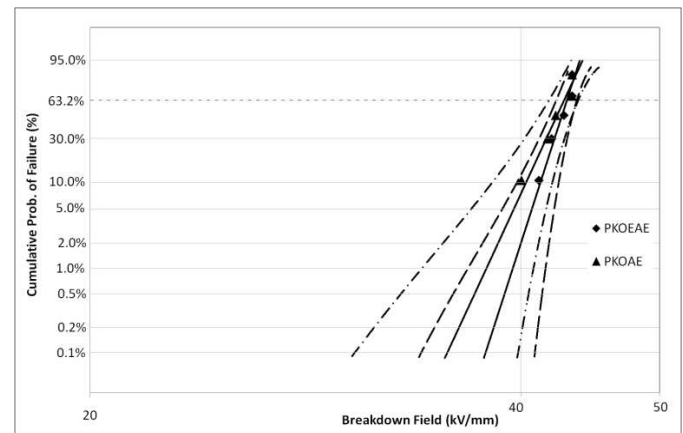


**Figure 13: Weibull distribution of palm kernel oil alkyl esters**

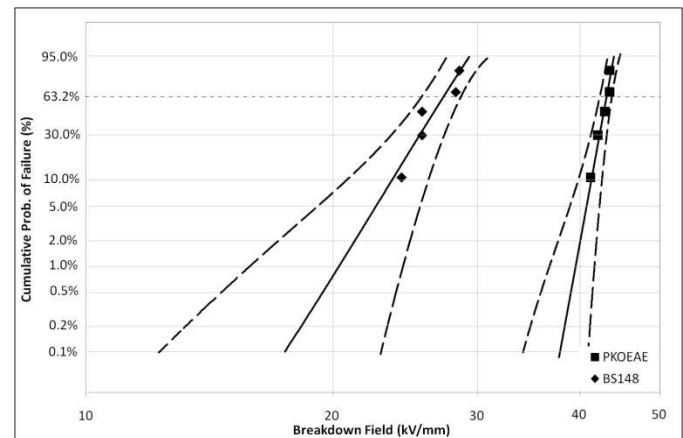


**Figure 14: Weibull distribution of mineral oil and PKOAE**

**Table 3 : Weibull Parameters of the Breakdown test**

Samples	N	Characteristic value, $\alpha$ (kV/mm)	95% Confidence Bound for $\alpha$ (kV/mm)	Shape parameter, $\beta$	95% Confidence Bound for $\beta$
BS148	5	27	25.83 - 28.83	15.49	8.82 - 37.17
CPKO	5	37	36.50 - 37.67	49.69	28.29 - 119.20
PPKO	5	41	39.92 - 42.73	23.05	13.13 - 55.31
PKOAE	5	43	41.88 - 43.71	42.90	20.94 - 88.22
PKOEA	5	43	42.37 - 43.65	52.58	30.09 - 126.78

Note: Values for CPKO and PPKO are at 30 °C, while the values for BS148, PKOAE and PKOEA are at 20 °C

The high values for the fitted shape parameter,  $\beta$ , found for palm kernel oil and the ester derivatives demonstrates good reproducibility of the measurement technique and that these oils have a narrow distribution of breakdown fields comparable to that found for mineral oil. Figures 11 through 14 show plots of the Weibull distributions obtained from the breakdown measurements for the different oil types at the different stages of preparation. In figure 11, the crude (CPKO) oil is compared with the purified oil (PPKO). Although the two distributions have different slopes, the characteristic breakdown strength (63.2% cumulative probability) of the purified oil is significantly higher. This could be due to reduced concentration of impurities and a reduction in the DC conductivity. This suggests that the impurities in CPKO may have aligned to form a bridge across the gap due to its attraction towards higher field region. This may have increased the field in the liquid within the gap, leading to breakdown after it reached critical value. Early onset of electrohydrodynamic instability due to high impurity level in the sample may also have contributed by initiating early breakdown. The Weibull distributions for the purified (PPKO) and the ester derivative (PKOAE) are compared in figure 12. No significant difference in the distribution was found following esterification. As demonstrated in figure 13, no significant difference was found in the Weibull distribution following epoxidation. In figure 14, the Weibull distribution of the epoxidized ester (PKOEA) is compared to that of mineral oil (BS148). Over the full range of failure probability, the breakdown strength of the epoxidized ester is significantly greater than for the mineral oil.

## 4 CONCLUSION

The purified sample shows a decrease in the overall dielectric loss compared with the crude oil sample. This is consistent with reduced electrical conductivity of the purified oil sample a factor of 10 lower than that of the crude oil sample. The electrical conductivity of the purified sample was found to be a factor of 10 higher than that of BS148 mineral oil. However further processing of the ester significantly increased the bulk conductivity due to increased concentration of mobile ions and reduced viscosity of the fluid. At high temperatures ~80°C and below a frequency dependent on the bulk conductivity of the fluid, there exist a drift of the charge carriers in the oil samples that forms an electric double layer at the electrode-liquid interface.

The mean breakdown voltage measurements on mineral oil

samples obtained using the new bespoke breakdown test cell was found to be comparable with literature values obtained using the ASTM standard. This confirms the validity of using the bespoke test cell for small sample volumes for breakdown strength measurements of the oil samples.

The characteristic breakdown field of the ester derivatives of palm kernel oil is about 37% higher than BS148 mineral oil. The statistical analysis of the electrical breakdown field data of palm kernel oil samples and its ester derivatives follow the Weibull distribution function. The increase in the characteristic breakdown field of the purified sample and the alkyl esters may be related to the low content of impurities after purification. The ester derivatives were found to have high shape parameters, indicating that the breakdown data has narrow distribution as good as or better than mineral oil. The results show that esters of palm kernel oil have improved electrical breakdown property and may be considered as an alternative base-stock for mineral oil insulation fluid. However, the high electrical conductivity of the processed oils could present a problem at high temperature and these materials could benefit from a further re-purifying stage to remove ionic impurities.

## 5 ACKNOWLEDGEMENTS

This study was supported by Islamic Development Bank under the IDB Merit Scholarship Programme for High Technology. It was also supported by National Grid, UK.

## 6 REFERENCES

1. M. Abdel-salam, H. Anis, A. El-Morshedy, R. Radwan, High Voltage Engineering: Theory and Practice, Mercel Dekker, Inc. New York, 2000.
2. A.A. Abdelmalik, A.P. Abbott, J.C. Fothergill, S. Dodd & R.C. Harris, "Synthesis of a Base-Stock for Electrical Insulating Fluid based on Palm Kernel Oil", Industrial Crops and Products, 33, 532–536, 2011.
3. ASTM D149-97a, Standard Test Method for Dielectric Breakdown Voltage and Dielectric Strength of Solid Electrical Insulating Materials at Commercial Power Frequencies, ASTM.
4. IEC 156:1995, Insulating Liquids – Determination of the Breakdown Voltage at Power Frequency – Test Method, IEC.
5. A.J. Bard, L.R. Faulkner, Electrochemical Methods; Fundamentals and Applications, Second Edition, John Wiley & Sons, Inc, 2001.

6. W.F. Schmidt, Conduction Mechanism in Liquids in Engineering Dielectric, Vol. III, Electrical Insulating Liquids, R. Bartnikas, p. 147-260, ASTM Publication, 1994.
7. W.S. Zaengl, Dielectric Spectroscopy in Time and Frequency Domain for HV Equipments, Part 1: Theoretical Considerations, IEEE Insulation magazine, Vol. 19, No. 5, 2003,
8. R. Bartnikas, Alternating-Current Loss and Permittivity Measurements in Engineering Dielectric, Vol. IIB, Electrical Properties of Solid Materials: Measurement techniques, R. Bartnikas, pp. 52-123, ASTM Publication, 1987.
9. R. Bartnikas, "Permittivity and Loss of Insulating Liquid" in Engineering Dielectrics, Vol. III, Electrical Insulating Liquids, R. Bartnikas, ASTM Publication, pp. 3-146, 1999.
10. H.A. Pohl, K. Pollock, J.S. Crane, Dielectrophoretic Force: A Comparison of Theory and Experiment, J. Biol Phys. Vol. 6, Pp. 133-160, 1978,
11. R. Arora, High Voltage Insulation Engineering, New Age International (P) Limited, Publishers, New Delhi, Pp. 223, 1995.
12. M. Butcher, A.A. Neuber, M.D. Cevallos, J.C. Dickens & H. Krompholz, Conduction and Breakdown Mechanisms in Transformer Oil, IEEE Trans. on Plasma Science, Vol. 34, No. 2. Pp. 467-475, 2006.
13. E.O. Forster, "Electrical Breakdown in Dielectric Liquid" in Engineering Dielectrics, Vol. III, Electrical Insulating Liquids, R. Bartnikas, Pp. 262-309, ASTM Publication, 1999.
14. E. Kuffel, W.S. Zaengl, J.Kuffel, High Voltage Engineering; Fundamentals, Newnes, Pp. 390-391, 2000.
15. L A Dissado, J C Fothergill, Electrical Degradation and Breakdown in Polymers, IEE, 1992.
16. D. Martin and Z.D. Wang, Statistical Analysis of the AC Breakdown Voltages of Ester Based Transformer Oils, IEEE Trans. on Dielectrics and Electrical Insulation, Vol. 15, No. 4, Pp. 1044-1050, 2008.
17. IEEE Std 930-2004, IEEE Guide for the Statistical Analysis of Electrical Insulation Breakdown Data, IEEE, 2005.
18. W.A. Welsh, Y.O. Parent, Method for Refining Glyceride Oils Using Amorphous Silica, United State Patent US 4,629,588, 1986.
19. J.H. Cloete, J. van der Merwe, The Breakdown Electric Field Strength Between Two Conducting Spheres by the Method of Images, IEEE Trans. on Education, Vol. 41, No. 2 Pp. 141-145, 1998.
20. A.K. Jonscher, "Dielectric relaxation in solids", Chelsea Dielectric Press, 1983.
21. T. Umemura, K. Akiyama, T. Kawasaki & T. Kashiwazaki, Electrical conduction in synthetic insulating liquid, IEEE Trans. on Electrical Insulation, Vol. EI-17, No. 6, Pp. 533-538, 1982.
22. C.T. Dervos, C.D. Paraskevas, P. Skafidas, P. Vassiliou, 2005, Dielectric Characterization of Power Oils as a Diagnostic life Prediction Method, IEEE Insulation Magazine, Vol. 21, No. 1.
23. IEEE Std C57.147-2008, IEEE Guide for Acceptance and Maintenance of Natural Ester Fluids in Transformers, IEEE.



**Abdelghaffar A. Abdelmalik** was born in Lagos, Nigeria in 1976. He graduated from Ahmadu Bello University, Zaria, Nigeria in 2000 with a B.Sc. degree in Physics. He also received a Master's degree in Physics in 2005 from the same institution. He is currently a PhD student in the Department of Engineering, University of Leicester, Leicester, UK. His research area is on Alternative Electrical Insulation Fluid for Transformers.

He is a Graduate Student Member of IEEE DEIS.



**John C. Fothergill (SM'95, F'04)** was born in Malta in 1953. He graduated from the University of Wales, Bangor, in 1975 with a Bachelor's degree in Electronics. He continued at the same institution, working with Pethig and Lewis, gaining a Master's degree in Electrical Materials and Devices in 1976 and doctorate in the Electronic Properties of Biopolymers in 1979. Following this he worked as a senior research engineer leading research in electrical power cables at

STL, Harlow, UK. In 1984 he moved to the University of Leicester as a lecturer. He now has a personal chair in Engineering and is currently Head of the Department of Engineering.



**S.J. Dodd** was born in Harlow, Essex in 1960. He received the B.Sc. (Hons) Physics degree in 1987 and the Ph.D. degree in physics in 1992, both from London Guildhall University, UK and remained at the University until 2002 as a Research Fellow. He joined the University of Southampton in 2002 as a Lecturer in the Electrical Power Engineering Group in the School of Electronics and Computer Science and then the University of Leicester in the Electrical Power and

Power Electronics Research Group in the Department of Engineering in 2007 as a Senior Lecturer. His research interests lie in the areas of light scattering techniques for the characterization of polymer morphology, electrical treeing breakdown process in polymeric materials and composite insulation materials, electroluminescence and its relationship with electrical and thermal ageing of polymers, characterization of liquid and solid dielectrics and condition monitoring and assessment of high voltage engineering plant. His research has attracted funding from the electrical generation and transmission industries. He has published 22 papers, 37 conference papers and contributed to two books.